



Cite this: RSC Adv., 2018, 8, 20048

## *In situ* monitoring of SI-ATRP throughout multiple reinitiations under flow by means of a quartz crystal microbalance†

Joydeb Mandal, R. S. Varunprasaath,<sup>ab</sup> Wenqing Yan,<sup>a</sup> Mohammad Divandari, Nicholas D. Spencer \*<sup>a</sup> and Matthias Dübner<sup>\*a</sup>

An investigation of the polymerisation of 2-hydroxyethyl methacrylate (HEMA) by means of surface-initiated atom transfer radical polymerisation (SI-ATRP) has been carried out *in situ* using a quartz crystal microbalance, with multiple reinitiations under continuous flow of the reaction mixture. The SI-ATRP kinetics of HEMA were studied continuously by means of changes in the frequency, varying conditions including temperature and solvent composition, as well as monomer and catalyst concentrations, showing the influence of key reaction parameters on SI-ATRP kinetics. Such experiments enabled the design of a polymerisation protocol that leads to a reasonably fast but well-controlled growth of poly(HEMA) brushes. Furthermore, only a minor change in growth rate was observed when the polymerisation was stopped and reinitiated multiple times (essential for block synthesis), demonstrating the living nature of the SI-ATRP reaction under such conditions. The clean switching of reaction mixtures in the flow-based QCM has been shown to be a powerful tool for real-time *in situ* studies of surface-initiated polymerisation reactions, and a promising approach for the precise fabrication of block-containing brush structures.

Received 10th April 2018  
Accepted 24th May 2018

DOI: 10.1039/c8ra03073a  
[rsc.li/rsc-advances](http://rsc.li/rsc-advances)

## Introduction

Growing polymer brushes from a surface is an attractive method for tailoring the physicochemical properties of an interface. These include adhesion, friction, wettability and biocompatibility.<sup>1</sup> Moreover, the use of surface-initiated reversible deactivation radical polymerization (SI-RDRP), also known as surface-initiated controlled radical polymerization (SI-CRP), for polymer-brush preparation can be considered as one of the major advances within this field, due to the excellent control it offers over both architecture and functionality.<sup>2</sup>

Atom transfer radical polymerisation (ATRP) has been extensively used in polymer-brush preparation due to its extremely robust and versatile nature.<sup>3</sup> Unfortunately, a thorough understanding of SI-RDRP kinetics has remained elusive due to a general lack of appropriate analytical tools to monitor the growth of polymer brushes in real time. The kinetic aspects of SI-RDRP have been principally studied *ex situ* by measuring the dry thickness of polymer brushes after various reaction times, using different surface-sensitive analytical methods (e.g. atomic force microscopy, ellipsometry).<sup>4,5</sup> As an alternative, free

initiator is commonly added to the reaction mixture, with the aim of studying SI-RDRP kinetics indirectly, making the assumption that the free polymers grown in solution resemble those grown from the surface.<sup>6,7</sup> In contrast to the polymer chains growing in solution, those growing from surfaces experience a drastic reduction in degrees of freedom, which can significantly influence their growth kinetics.<sup>8,9</sup> The effect of surface grafting on ATRP kinetics has been studied by degrafting the polymer chains from surfaces using initiators that are capable of undergoing on-demand bond-fission.<sup>10–12</sup> Recently, Kang *et al.*<sup>13</sup> used a photo-cleavable SI-ATRP initiator to observe that the molar mass of the detached polymer chains was relatively lower than that of the polymers grown in solution, as a consequence of surface-induced crowding<sup>8</sup> and early chain termination.<sup>9</sup> Others have shown that under some circumstances, the surface-bound chains can actually have higher molar mass than their solution-grown counterparts.<sup>14</sup> Nevertheless, although useful, this approach also represents a *post mortem* analysis, and cannot provide insights into the kinetics (and changes thereof) during the growth process.

Thus, there remains a need for a robust and versatile analytical technique, capable of monitoring the growth of polymer brushes in real time. Commonly used for studies of interfacial processes<sup>15</sup> or biomolecular interactions,<sup>16,17</sup> the quartz crystal microbalance (QCM) has potential in this regard because of its ability to monitor changes in added mass in real time,<sup>18</sup> yielding details about the properties of the film grown on

<sup>a</sup>Laboratory for Surface Science and Technology, Department of Materials, ETH Zurich, Vladimir-Prelog-Weg 5, CH-8093 Zurich, Switzerland. E-mail: nspencer@ethz.ch

<sup>b</sup>Indian Institute of Science, Bangalore, India

† Electronic supplementary information (ESI) available. See DOI: [10.1039/c8ra03073a](https://doi.org/10.1039/c8ra03073a)



the sensor surface.<sup>19,20</sup> In the past decade, the instrument has gained increased attention from polymer scientists, who have utilized it to follow conformational changes<sup>21,22</sup> or the sensor potential<sup>23</sup> of grafted polymer chains. QCM has also been used to study the real-time growth of polymer brushes using surface-initiated polymerisation.<sup>24–29</sup> The applicability of QCM in understanding the effect of various reaction parameters such as monomer structure,<sup>27</sup> initiator density<sup>25,26</sup> and Cu(I)/Cu(II)<sup>28</sup> ratio on the SI-ATRP kinetics has been effectively demonstrated over the last decade. Notably, the need for a continuous flow through the confined cell environment to exclude concentration effects during the progress of polymerisation was demonstrated by Ma and coworkers.<sup>26,27</sup> However, many questions still need to be answered to gain a clear understanding of the complex characteristics of SI-ATRP. QCM has been utilized previously in our laboratory to monitor polymer-brush growth by means of photo-initiator-mediated polymerisation<sup>30</sup> and various grafting-to systems<sup>31</sup> but the focus of these studies was on understanding film structure and solvation.

Here we present a kinetic study of the SI-ATRP of 2-hydroxyethyl methacrylate (HEMA) by exploiting the mass-frequency relationships in QCM, whereby the increase in adsorbed mass can be directly related to the adsorbed combined mass of both

brush and trapped solvent and hence to polymer-brush growth. Experiments were typically carried out under a continuous flow of reaction mixture using a flow module coupled with a multi-position selection valve for a clean switching of reaction mixtures without affecting the flow. Furthermore, the effect of continuous flow on the polymerization kinetics was examined by carrying out the polymerization with and without flow. The influence of various reaction parameters such as temperature, monomer and catalyst concentration were examined in detail to understand the polymerization kinetics. In this way, polymerization protocols could be designed that offer excellent control over polymer-brush growth, as demonstrated by the linear decrease in frequency as a function of polymerization time. Multiple reinitiation with the same monomer, *i.e.* the synthesis of homoblock systems, was examined, so as to eliminate the effects of monomer-dependent kinetic variation, and to be able to focus on the issues of reinitiation and switching. The applicability of QCM in layered-structure fabrication was demonstrated *via* the formation of homopolymer blocks upon multiple reinitiations, which could be performed without any significant loss in reactivity. This is an essential first step before heteroblock structure synthesis can be contemplated.

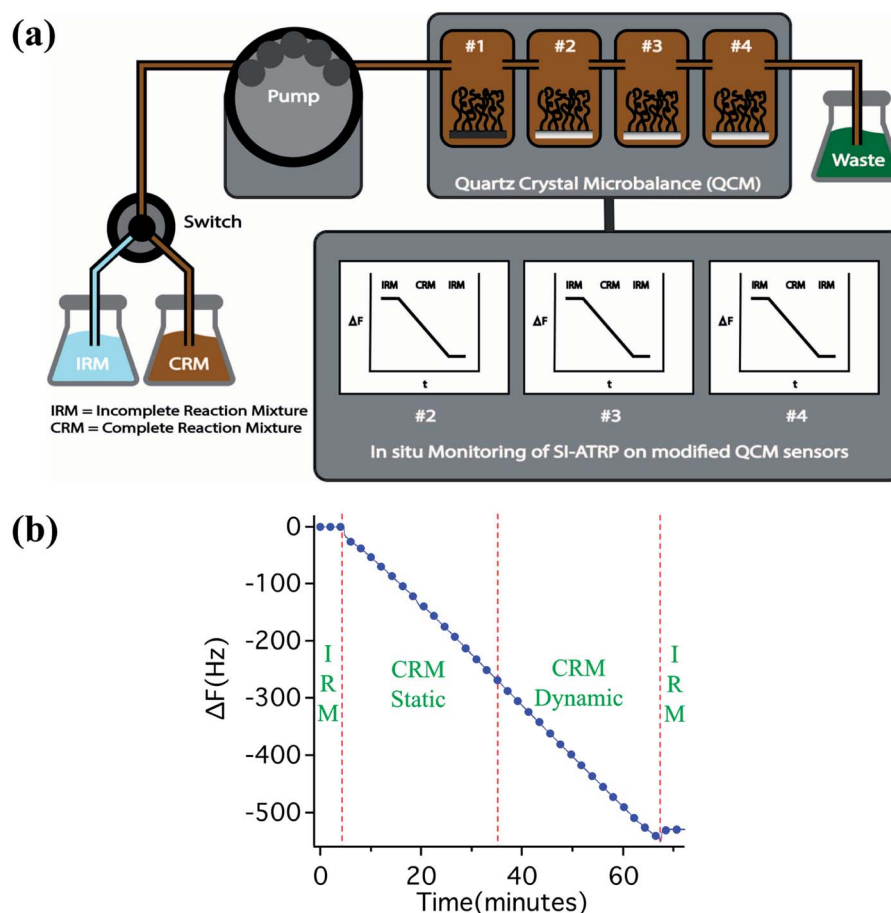


Fig. 1 (a) QCM flow setup used for the *in situ* SI-ATRP kinetic study of HEMA polymer-brush growth in water. The black substrate in cell #1 represents the dummy sensor (ATRP-initiator-modified Si wafer, cut into the shape and size of a QCM sensor) (b) frequency changes measured *in situ* by QCM during SI-ATRP of 1 : 1 HEMA/water mixture at 25 °C, first without catalyst, then with catalyst, in both the absence (static) and presence (dynamic) of flow, and then without catalyst again.



**Table 1** Dry and swollen thicknesses in Milli-Q water of polymer brushes, prepared with different catalyst concentrations and 1 : 1 HEMA/water mixture, as measured by both AFM and ellipsometry at room temperature

Catalyst conc. (%)	AFM (dry thickness, nm)	AFM (swollen thickness, nm)	Ellipsometry (dry thickness, nm)	Ellipsometry (swollen thickness, nm)	AFM swelling ratio <sup>a</sup>	Ellipsometry swelling ratio <sup>a</sup>
40	22	27	30 ± 2	57 ± 4	1.2	1.9
70	46	61	55 ± 3	88 ± 3	1.3	1.6
100	48	60	58 ± 4	87 ± 5	1.3	1.5

<sup>a</sup> Swelling ratio defined as  $T_{\text{swollen}}/T_{\text{dry}}$ .

## Results and Discussion

Immobilisation of a SI-ATRP initiator onto QCM sensors was carried out in a similar way to a previously established procedure.<sup>32</sup> In brief,  $\alpha$ -bromo isobutyl bromide was conjugated to a monolayer of (3-aminopropyl)triethoxysilane on  $\text{SiO}_2$ -coated QCM sensors. The modified sensors were placed inside QCM flow-cells and an incomplete (catalyst-free) reaction mixture (IRM; *i.e.* HEMA + water + ligand) was flowed through them at a rate of 10 mL h<sup>-1</sup> using a peristaltic pump. After the establishment of a stable baseline, the medium was switched from the IRM to the complete reaction mixture (CRM; *i.e.* IRM + catalyst) using a multi-position selection valve to initiate the polymerisation. The reaction was allowed to proceed for one hour and was terminated by switching the reaction medium back to IRM. A supplementary cell was placed in series with the working QCM cells, carrying a dummy sensor (an ATRP-initiator-modified Si wafer, cut into the shape and size of a QCM sensor), in order to perform additional *post mortem* characterisation by means of atomic force microscopy (AFM), ellipsometry and FTIR spectroscopy. A schematic illustration of the experimental setup is presented in Fig. 1a.

Although SI-ATRP has previously been carried out within a QCM under flow, the influence of flow on the reaction kinetics has not been reported.<sup>26,27</sup> In order to address this issue, which is crucial for any subsequent application in block-copolymer fabrication, SI-ATRP was carried out in CRM for 30 minutes under static conditions and then continued for another 30 minutes under a flow of 10 mL h<sup>-1</sup> with CRM and *vice versa*. For these experiments, IRM solutions were prepared by dissolving the ligand (2,2'-bipyridyl, bpy) in a 1 : 1 HEMA/water mixture, while the CRM solutions were prepared by dissolving CuCl and CuBr<sub>2</sub> into IRM solution. The growth of polymer brushes was monitored *in situ* by the change in frequency, as measured by QCM. A linear decrease in frequency ( $-\Delta F$ ) was observed, indicative of an increase in effective mass with time due to increasing polymer-brush thickness. The reaction profile did not show a difference when the system was switched from the static (without flow) to the dynamic (with flow) mode. This clearly establishes the potential of the flow system for monitoring many interesting processes, such as layered-structure formation and post-polymerisation modification. The controlled nature of any ATRP process is a result of the equilibrium between dormant polymer chains and active radical

species. Therefore, any environmental factor (such as solvent, monomer, initiator and temperature) that can influence this equilibrium is critically important in understanding the reaction kinetics. To gain a better understanding of SI-ATRP kinetics, the effect of the catalyst concentration on the SI-ATRP kinetics in a 1 : 1 HEMA/water mixture was studied at 25 °C in a range of 40–100% relative catalyst concentration. The exact catalyst composition of the various reaction mixtures are presented in the SI (Table 1). The segments of the  $\Delta F$ -*t* plots representing the propagation of the polymerisation are presented in Fig. 2a (full data shown in the ESI†). In all cases a steady linear decrease in frequency ( $-\Delta F$ ) was observed as a function of the polymerisation time, representing a linear increase in effective mass, indicating a controlled growth of grafted polymer chains. The slope of the  $\Delta F$ -*t* plots was in general found to increase upon increasing catalyst concentration, representing an increase in the overall rate of polymerisation. However, this effect was found to diminish somewhere above 70% catalyst concentration. This diminishing effect of catalyst concentration on the SI-ATRP kinetics could be the result of Cu<sup>I</sup>-induced catalytic radical termination.<sup>33</sup>

In addition, *ex situ* characterisation of the grafted polymer brushes was carried out using FTIR spectroscopy, ellipsometry and AFM (Table 1 and ESI†). Both the dry and swollen thicknesses of the polymer brushes, measured by ellipsometry and AFM, exhibited a significant increase when the catalyst concentration was increased from 40 to 70% but the increase was less significant upon increasing the concentration from 70 to 100%, which is consistent with the QCM kinetic study (Fig. 2a). It should be noted that the dry and swollen thickness values measured by AFM were lower than those measured by ellipsometry, which could be due to the compression of the coatings by the AFM tip during measurement.<sup>34</sup>

The temperature of the reaction medium is clearly another factor that will greatly influence the overall kinetics of ATRP.<sup>35</sup> In order to understand the effect of reaction temperature on the SI-ATRP kinetics, the reaction was performed at 25 °C, 35 °C and 45 °C (at a relative 100% catalyst concentration) using a 7 : 3 HEMA/water mixture (Fig. 2b)—chosen for its slow and well-controlled polymerisation profile (Fig. 3), which will be discussed in detail in the following section. The segments of the  $\Delta F$ -*t* plots representing the progress of the polymerisation are presented in Fig. 2b. A more rapid decrease in frequency, demonstrating faster growth of the polymer brush as a function



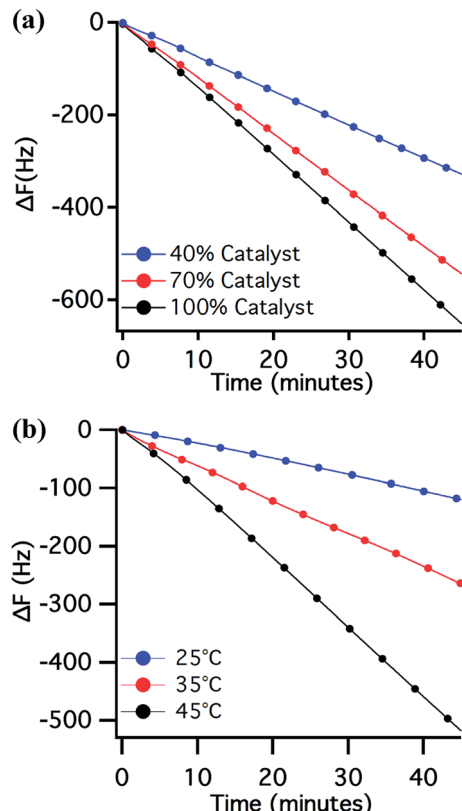


Fig. 2 Frequency variation measured in real time by QCM during SI-ATRP carried out under continuous flow of CRM, with different relative catalyst concentrations and 1 : 1 HEMA/water mixture at 25 °C (a), and at different reaction temperatures with 100% relative catalyst concentrations and 7 : 3 HEMA/water mixture (b).

of time, was observed with an increase in reaction temperature. Despite the strong reaction-rate enhancement, the linear  $\Delta F$ - $t$  relation in all three cases demonstrated the existence of controlled SI-ATRP throughout our working temperature range.

In a second study, the effect of monomer concentration on the polymer-brush growth was examined by carrying out experiments with a varying HEMA-to-water ratio (v/v) from 7 : 3 to 3 : 7, while maintaining other reactant concentrations unchanged (at a relative 100% catalyst concentration and 25 °C). The growth of the polymer brushes was monitored *in situ* by QCM in all cases and the polymerisation segments of the  $\Delta F$ - $t$  plots are presented in Fig. 3 (full data shown in the ESI†). Two points emerge from the comparison of the polymerisation profiles: (i) the rate at which the frequency drops, increasing with decreasing monomer concentration or with increasing relative water content in the reaction mixture, indicates a faster rate of polymerisation; (ii) the linear decrease in frequency, representing a controlled growth of polymer brushes, was observed when the polymerisation was carried out at HEMA to water ratios of 7 : 3 and 1 : 1. However, this linearity was lost when SI-ATRP was performed with a 3 : 7 HEMA/water mixture, indicating the loss of control of polymer-brush growth.

To better understand this phenomenon, we studied the growth of the polymer brushes *ex situ* by measuring the dry thickness of the grafted thin films at different times by means of

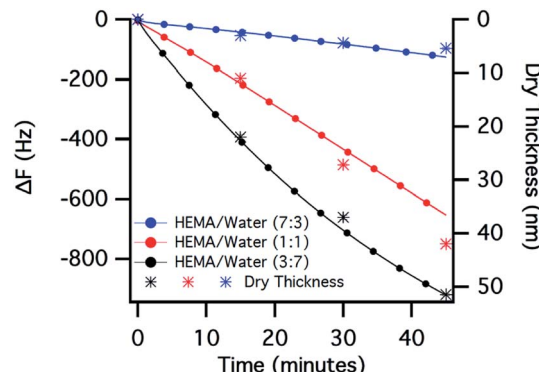


Fig. 3 SI-ATRP of HEMA at 25 °C with different relative monomer concentrations and 100% relative catalyst concentration, studied by recording the frequency change in real time using QCM. The dry thickness (error bars within the range of 0.1 to 0.5 nm) of the polymer brushes measured *ex situ* by ellipsometry at different times are overlaid with the  $\Delta F$ - $t$  plots in the corresponding colours.

ellipsometry. The *ex situ* study also exhibited a similar trend, in which the dry thickness increased with an increase in relative water content in the reaction mixture, as shown in Fig. 3. Considering zero brush thickness at the onset of polymerisation, a nonlinearity could be seen in the case of 7 : 3 HEMA/water mixture while the linearity is maintained in the other two cases, as was observed when polymerisation was performed *in situ* (Fig. 3). Similar water-induced acceleration for SI-ATRP has also been observed by others when growing poly(HEMA) brushes from a gold surface.<sup>36</sup> In 2004, Matyjaszewski *et al.*<sup>37,38</sup> demonstrated that ATRP reactions are usually fast in aqueous media and exhibit a dramatic acceleration, associated with a loss of control, when the water content in the reaction mixture was increased. The accelerated kinetics were attributed to the inefficient deactivation of the active radicals, due to a displacement of the halide ligands from the ATRP deactivator Cu(II)L<sub>n</sub>X by water molecules. Thus, it is reasonable to assume that the effect of the relative amount of water in the medium outweighs the effect of monomer concentration, resulting in an increase in the polymerisation rate, even though the monomer concentration was reduced.

In addition to its control over both molar mass and dispersity, one very important feature of ATRP is its ability to undergo multiple reinitiation steps, which in turn allows the formation of a variety of complex macromolecular architectures with diverse compositions.<sup>39–43</sup> This feature of ATRP has also been demonstrated for SI-ATRP by others to construct block-copolymer brushes from a number of different surfaces.<sup>44–46</sup> However, the present flow system clearly has some advantages over previous work thanks to the possibility of clean switching between monomer mixtures without affecting the polymerization process. Specifically, in previous studies, reinitiation was performed by stopping the reaction, cleaning the polymer film, drying and analyzing the surface, followed by further initiations. This can result in new chain growth from the unreacted initiators remaining on the surface.<sup>47</sup>

In order to have a clearer understanding about the reinitiation efficiency of SI-ATRP, an experiment using 1 : 1 HEMA/



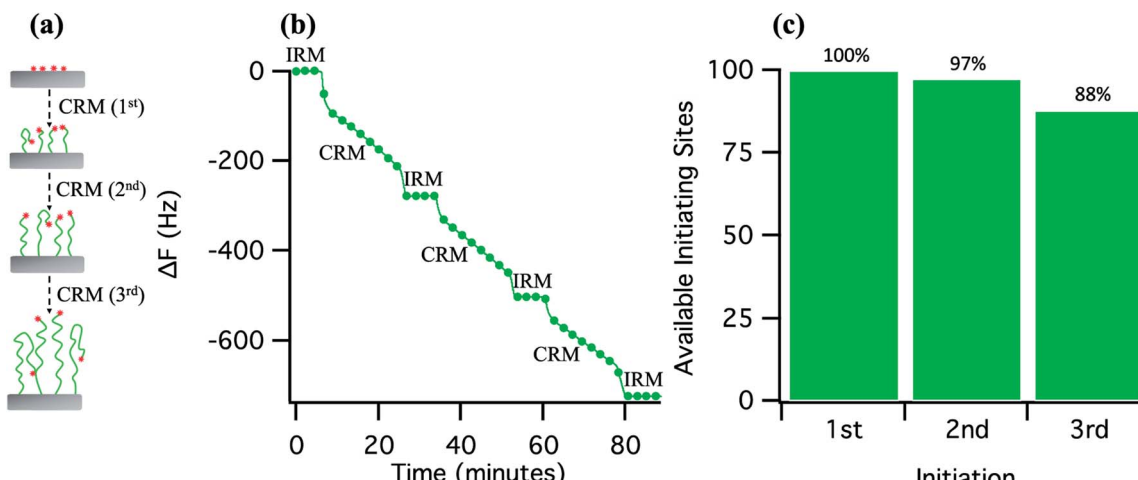


Fig. 4 Schematic illustration of the block-wise growth of poly(HEMA) brush due to multiple initiations and terminations (a). Multiple initiations and terminations, caused by repeated switching of CRM and IRM solutions, recorded *in situ* by QCM during SI-ATRP of 1 : 1 HEMA/water mixture with 100% relative catalyst concentration at 25 °C (b). Available initiating sites calculated from the slopes of the polymerization profiles after each initiation (c).

water mixture (at a relative catalyst concentration of 100% and 25 °C reaction temperature) was carried out where the polymerisation was interrupted and reinitiated multiple times by switching the CRM solution to IRM solution and *vice versa*, resulting in a staircase-like growth profile in the QCM plot (Fig. 4b). The CRM solution at each step was injected only after a stable baseline was established with the IRM solution. A monotonic, linear decrease in the frequency as a function of time, observed at each step of polymerisation, demonstrates a controlled growth of polymer brush at each stage. More interestingly, repeated cycles of interruption and initiation produced very similar polymerisation profiles without any significant decrease in the rate of polymerisation (the slope of the polymerisation profiles changed from 7.57 to 7.38 to 6.65). Since the reactant concentrations were maintained unchanged at each initiation stage by flowing the same CRM solution, the observed change in the rate of polymerisation could be related to the loss of available initiating sites (Fig. 4c) due to the sudden termination of active radical centers upon interruption of the polymerization process, caused by a sudden dilution of Cu(II)X<sub>2</sub> upon replacement of CRM with IRM. Most importantly, the availability of the initiating sites was close to 90% at the 3<sup>rd</sup> initiation. This high degree of initiation-site preservation for SI-ATRP after interruption under continuous flow is higher than values previously reported by Kim *et al.*<sup>46</sup> (85–90%) under stagnant conditions.

## Conclusion

QCM was employed in this study to examine the effect of various reaction parameters on the growth kinetics of poly(HEMA)-brushes prepared, continuously or with reinitiations, by SI-ATRP from modified SiO<sub>2</sub>-coated quartz crystals. The time-resolved mass-frequency correlations, obtained from QCM measurements of SI-ATRP carried out at different temperatures, catalyst concentration, monomer concentration, and solvent

polarity, provided an insight into the kinetics of SI-ATRP and helped in choosing reaction parameters for rapid, well-controlled brush growth. The inclusion of the additional switching valve in the flow module facilitated multiple initiations and terminations and hence the construction of homo-polymer blocks (and by extension, the potential for block-copolymer synthesis) by switching the reaction mixtures. This approach, together with QCM's utility for studying SI-RDRP kinetics *in situ* makes it a powerful tool for designing polymerization protocols for the controlled growth of multiblock polymer-brush architectures.

## Experimental section

### Materials

α-Bromoisobutyryl bromide (98%), (3-aminopropyl)triethoxysilane (97%), dichloromethane (99.8%, extra dry), triethylamine (≥99.5%), copper(II) bromide (99%), 2,2'-bipyridyl (≥99%) were purchased from Sigma Aldrich (Germany) and used as received. 2-Hydroxyethyl methacrylate (≥99%) was purchased from Sigma Aldrich (Germany) and passed through a basic alumina column before use, to remove the hydroquinone inhibitor. Cu(I) chloride was purchased from Sigma Aldrich and was purified by stirring overnight in glacial acetic acid, filtered, washed several times with acetone, and finally dried under vacuum. Silicon wafers (P/B < 100) were purchased from Si-Mat Silicon Wafers (Germany) and SiO<sub>2</sub>-coated QCM sensors were purchased from Q-Sense (Sweden).

### Methods

**Immobilisation of ATRP initiator.** SiO<sub>2</sub>-coated sensors and the Si-wafers were cleaned by sonicating them for 10 minutes each in toluene and isopropanol, followed by ozone treatment (UV/Ozone ProCleanerTM and ProCleanerTM Plus, BioForce, (USA)) for 35 minutes. The UV-treated samples and 0.1 mL (3-aminopropyl)triethoxysilane were then placed inside



a desiccator, which was evacuated for one hour using a high-vacuum pump. The vacuum was maintained for an additional two hours after the pump had been switched off. The substrates were then washed with toluene, dried under  $N_2$  and placed inside an Erlenmeyer flask equipped with a rubber septum. The flask was then purged with  $N_2$  gas for 5 minutes and then charged with 10 mL dry DCM, 0.1 mL triethylamine and 0.1 mL  $\alpha$ -bromo isobutyryl bromide and kept under argon atmosphere for 3 hours. Finally, the substrates were washed with DCM, dried under  $N_2$  gas and used to carry out SI-ATRP.

#### Surface-initiated atom transfer radical polymerisation

(a) *SI-ATRP inside QCM.* To prepare the IRM solution, 762.5 mg of 2,2'-bipyridyl (bpy) was dissolved in 25 mL 1 : 1 HEMA/water mixtures and deoxygenated by bubbling nitrogen gas for 30 minutes. After that, 15 mL of the IRM solution were transferred to a flask kept under  $N_2$  and containing 103.2 mg CuCl (1.032 mmol) and 67 mg CuBr<sub>2</sub> (0.298 mmol). This catalyst concentration is designated to be 100% with respect to the total volume of the CRM solution, and in some experiments the concentration was varied. This solution was then stirred for another 30 min to allow the formation of the catalyst complex—characterised by the formation of a dark-brown solution. The QCM flow cells equipped with the initiator-modified, SiO<sub>2</sub>-coated sensors and the dummy sensor were then charged with the IRM solution with a constant flow rate of 10 mL h<sup>-1</sup>. As soon as a stable baseline was established, the polymerisation was initiated by switching the medium from IRM to CRM using a multi-position selection valve (Vici, model no.: EUHA, Serial no.: EUA08048, Valco Instruments, Houston, Texas, USA) and finally the polymerisation was stopped by switching back to IRM. Finally, the sensors and the Si-wafer (dummy sensor) were taken out of the cell, washed several times with water, ethanol and dried under a  $N_2$  stream.

The effect of monomer concentration was studied by carrying out SI-ATRP at 25 °C in 7 : 3, 1 : 1 and 3 : 7 HEMA/water mixtures. In all cases, the amount of ligand and catalyst (100%) were kept similar with respect to the total volume of the reaction mixture. The effect of catalyst concentration was studied by performing SI-ATRP at 25 °C with a 1 : 1 HEMA/water mixture. The concentration of ligand and catalyst was varied from 100 to 40% with respect to the total volume of the reaction mixture. Similarly, the effect of temperature was studied with 7 : 3 HEMA/water mixture at 100% catalyst loading, where the temperature was varied from 25 to 45 °C.

(b) *SI-ATRP from Si wafers.* The CRM solution was transferred to the flasks kept under  $N_2$  and containing initiator-modified Si-wafers, in order to initiate the polymerisation. The polymerisation was carried out for different lengths of time and finally the substrates were taken out, washed several times with Milli-Q water, ethanol and dried under a  $N_2$  stream and finally used for further experiments.

#### Characterisation

To obtain infrared spectra, poly(HEMA)-modified silicon wafer samples were measured on a Vertex 70 FT-IR microscope (Bruker, Fällanden, Switzerland) with a spectral range of

4000 cm<sup>-1</sup> to 375 cm<sup>-1</sup> under a continuous flow of nitrogen. Reference spectra were recorded just prior to the actual measurement. OPUS spectroscopy software (version 6.5, Bruker, Fällanden, Switzerland) was used for data processing.

Variable-angle spectroscopic ellipsometry, (VASE) M-2000F (LOT Oriel GmbH, Darmstadt, Germany) was used to measure polymer film thicknesses, both in air and in Milli-Q water, using a custom-built liquid cell. Determination of  $\Psi$  and  $\Delta$  as a function of wavelength (275–827 nm) was carried out by employing the WVASE32 software package (LOT Oriel GmbH, Darmstadt, Germany). The brush-supporting substrates were in all cases considered as consisting of silicon with a 2 nm-thick silicon dioxide film. The analysis of the brush layers was performed on the basis of a Cauchy model:  $n = A + B\lambda^{-2}$  where  $n$  is the refractive index,  $\lambda$  is the wavelength and  $A$  and  $B$  were assumed to be 1.45 and 0.01, respectively, as values for transparent organic films.

For measuring the thickness of the films in water, the swollen poly(HEMA) layer was fitted by a two-component effective-medium-approximation (EMA) model, consisting of a Cauchy and a water component. In this medium, a layered model (Si/SiO<sub>2</sub>/EMA-poly(HEMA)/water-ambient) was used to determine the swollen thickness of the POEGMA layer. In this case, fitting was performed by considering thickness ( $T$ ), and water content ( $w$ ) of the EMA-POEGMA layer as fitting parameters.

AFM step-height images of coatings were taken using a Bruker Icon Dimension in air and Milli-Q water using TappingMode® and PeakForce® tapping modes respectively. For tapping-mode images an Olympus-OMCL-AC160TS-C3 (Japan) cantilever with a spring constant of 26 N m<sup>-1</sup> was used. For Peakforce mode a Bruker-SNL-10 tip with a spring constant of 0.35 N m<sup>-1</sup> was used. The dry and swollen thickness of the poly(HEMA) brushes were measured by mechanically removing the films using plastic tweezers and subsequently measuring the step height between brushes and the underlying, bare substrate.

QCM (Q-Sense E4 instrument, Västra Frölunda, Sweden) equipped with Q-Soft 301 software (Q-Sense AB, Göteborg, Sweden) was used to monitor the growth kinetics of *p*-HEMA brushes from SiO<sub>2</sub> coated sensors in real time. The instrument was coupled with a multi-position selection valve (Vici, model no.: EUHA, Serial no.: EUA08048, Valco Instruments, Houston, Texas, USA) and a peristaltic pump (Ismatec, Model no.: ISM827B, Serial no.: 0596214-1, Wertheim, Germany) to allow clean switching of the reaction mixtures.

#### Conflicts of interest

There are no conflicts to declare.

#### Acknowledgements

We gratefully acknowledge funding from the European Research Council (ERC) under the European Union's Horizon 2020 research and innovation programme (grant agreement No 669562).



## References

1 O. Azzaroni, Polymer brushes here, there, and everywhere: Recent advances in their practical applications and emerging opportunities in multiple research fields, *J. Polym. Sci., Part A: Polym. Chem.*, 2012, **50**(16), 3225–3258.

2 J. O. Zoppe, N. C. Ataman, P. Mocny, J. Wang, J. Moraes and H.-A. Klok, Surface-initiated controlled radical polymerization: state-of-the-art, opportunities, and challenges in surface and interface engineering with polymer brushes, *Chem. Rev.*, 2017, **117**(3), 1105–1318.

3 K. Matyjaszewski, Atom transfer radical polymerization (ATRP): current status and future perspectives, *Macromolecules*, 2012, **45**(10), 4015–4039.

4 D. Xiao and M. J. Wirth, Kinetics of surface-initiated atom transfer radical polymerization of acrylamide on silica, *Macromolecules*, 2002, **35**(8), 2919–2925.

5 J. B. Kim, W. Huang, M. D. Miller, G. L. Baker and M. L. Bruening, Kinetics of surface-initiated atom transfer radical polymerization, *J. Polym. Sci., Part A: Polym. Chem.*, 2003, **41**(3), 386–394.

6 T. von Werne and T. E. Patten, Atom transfer radical polymerization from nanoparticles: a tool for the preparation of well-defined hybrid nanostructures and for understanding the chemistry of controlled/“living” radical polymerizations from surfaces, *J. Am. Chem. Soc.*, 2001, **123**(31), 7497–7505.

7 J. Pyun, S. Jia, T. Kowalewski, G. D. Patterson and K. Matyjaszewski, Synthesis and characterization of organic/inorganic hybrid nanoparticles: kinetics of surface-initiated atom transfer radical polymerization and morphology of hybrid nanoparticle ultrathin films, *Macromolecules*, 2003, **36**(14), 5094–5104.

8 C. B. Gorman, R. J. Petrie and J. Genzer, Effect of substrate geometry on polymer molecular weight and polydispersity during surface-initiated polymerization, *Macromolecules*, 2008, **41**(13), 4856–4865.

9 J. Genzer, In silico polymerization: Computer simulation of controlled radical polymerization in bulk and on flat surfaces, *Macromolecules*, 2006, **39**(20), 7157–7169.

10 R. R. Patil, S. Turgman-Cohen, J. i. Šrogl, D. Kiserow and J. Genzer, On-demand degrafting and the study of molecular weight and grafting density of poly (methyl methacrylate) brushes on flat silica substrates, *Langmuir*, 2015, **31**(8), 2372–2381.

11 R. R. Patil, S. Turgman-Cohen, J. i. Šrogl, D. Kiserow and J. Genzer, Direct measurement of molecular weight and grafting density by controlled and quantitative degrafting of surface-anchored poly (methyl methacrylate), *ACS Macro Lett.*, 2015, **4**(2), 251–254.

12 S. Hansson, P. Antoni, H. Bergenudd and E. Malmström, Selective cleavage of polymer grafts from solid surfaces: assessment of initiator content and polymer characteristics, *Polym. Chem.*, 2011, **2**(3), 556–558.

13 C. Kang, R. Crockett and N. D. Spencer, The influence of surface grafting on the growth rate of polymer chains, *Polym. Chem.*, 2016, **7**(2), 302–309.

14 M. Husseman, E. E. Malmström, M. McNamara, M. Mate, D. Mecerreyes, D. G. Benoit, J. L. Hedrick, P. Mansky, E. Huang and T. P. Russell, Controlled synthesis of polymer brushes by “living” free radical polymerization techniques, *Macromolecules*, 1999, **32**(5), 1424–1431.

15 D. A. Buttry and M. D. Ward, Measurement of interfacial processes at electrode surfaces with the electrochemical quartz crystal microbalance, *Chem. Rev.*, 1992, **92**(6), 1355–1379.

16 A. Arnau, A review of interface electronic systems for AT-cut quartz crystal microbalance applications in liquids, *Sensors*, 2008, **8**(1), 370–411.

17 C. I. Cheng, Y.-P. Chang and Y.-H. Chu, Biomolecular interactions and tools for their recognition: focus on the quartz crystal microbalance and its diverse surface chemistries and applications, *Chem. Soc. Rev.*, 2012, **41**(5), 1947–1971.

18 D. Johannsmann, Viscoelastic, mechanical, and dielectric measurements on complex samples with the quartz crystal microbalance, *Phys. Chem. Chem. Phys.*, 2008, **10**(31), 4516–4534.

19 E. S. Dehghani, N. D. Spencer, S. N. Ramakrishna and E. M. Benetti, Crosslinking polymer brushes with ethylene glycol-containing segments: Influence on physicochemical and antifouling properties, *Langmuir*, 2016, **32**(40), 10317–10327.

20 J. Iruthayaraj, G. Olanya and P. M. Claesson, Viscoelastic Properties of Adsorbed Bottle-brush Polymer Layers Studied by Quartz Crystal Microbalance – Dissipation Measurements, *J. Phys. Chem. C*, 2008, **112**(38), 15028–25036.

21 G. Zhang and C. Wu, Quartz crystal microbalance studies on conformational change of polymer chains at interface, *Macromol. Rapid Commun.*, 2009, **30**(4–5), 328–335.

22 J. J. I. Ramos and S. E. Moya, Water content of hydrated polymer brushes measured by an *in situ* combination of a quartz crystal microbalance with dissipation monitoring and spectroscopic ellipsometry, *Macromol. Rapid Commun.*, 2011, **32**(24), 1972–1978.

23 N. Schüwer and H. A. Klok, A Potassium-Selective Quartz Crystal Microbalance Sensor Based on Crown-Ether Functionalized Polymer Brushes, *Adv. Mater.*, 2010, **22**(30), 3251–3255.

24 Y. Nakayama and T. Matsuda, In situ observation of dithiocarbamate-based surface photograft copolymerization using quartz crystal microbalance, *Macromolecules*, 1999, **32**(16), 5405–5410.

25 S. E. Moya, A. A. Brown, O. Azzaroni and W. T. Huck, Following polymer brush growth using the quartz crystal microbalance technique, *Macromol. Rapid Commun.*, 2005, **26**(14), 1117–1121.

26 H. Ma, M. Textor, R. L. Clark and A. Chilkoti, Monitoring kinetics of surface initiated atom transfer radical polymerization by quartz crystal microbalance with dissipation, *Biointerphases*, 2006, **1**(1), 35–39.

27 J. He, Y. Wu, J. Wu, X. Mao, L. Fu, T. Qian, J. Fang, C. Xiong, J. Xie and H. Ma, Study and Application of a Linear Frequency– Thickness Relation for Surface-Initiated Atom



Transfer Radical Polymerization in a Quartz Crystal Microbalance, *Macromolecules*, 2007, **40**(9), 3090–3096.

28 N. Cheng, O. Azzaroni, S. Moya and W. T. Huck, The effect of  $[\text{Cu(I)}]/[\text{Cu(II)}]$  ratio on the kinetics and conformation of polyelectrolyte brushes by atom transfer radical polymerization, *Macromol. Rapid Commun.*, 2006, **27**(19), 1632–1636.

29 L. Carlsson, S. Utsel, L. Wågberg, E. Malmström and A. Carlmark, Surface-initiated ring-opening polymerization from cellulose model surfaces monitored by a Quartz Crystal Microbalance, *Soft Matter*, 2012, **8**(2), 512–517.

30 R. Heeb, R. M. Bielecki, S. Lee and N. D. Spencer, Room-temperature, aqueous-phase fabrication of poly(methacrylic acid) brushes by UV-LED-induced, controlled radical polymerization with high selectivity for surface-bound species, *Macromolecules*, 2009, **42**(22), 9124–9132.

31 M. T. Müller, X. Yan, S. Lee, S. S. Perry and N. D. Spencer, Lubrication properties of a brushlike copolymer as a function of the amount of solvent absorbed within the brush, *Macromolecules*, 2005, **38**(13), 5706–5713.

32 C. Kang, S. N. Ramakrishna, A. Nelson, C. V. Cremmel, H. Vom Stein, N. D. Spencer, L. Isa and E. M. Benetti, Ultrathin, freestanding, stimuli-responsive, porous membranes from polymer hydrogel-brushes, *Nanoscale*, 2015, **7**(30), 13017–13025.

33 Y. Wang, N. Soerensen, M. Zhong, H. Schroeder, M. Buback and K. Matyjaszewski, Improving the “livingness” of ATRP by reducing Cu catalyst concentration, *Macromolecules*, 2013, **46**(3), 683–691.

34 S. N. Ramakrishna, M. Cirelli, M. Divandari and E. M. Benetti, Effects of Lateral Deformation by Thermoresponsive Polymer Brushes on the Measured Friction Forces, *Langmuir*, 2017, **33**(17), 4164–4171.

35 F. Seeliger and K. Matyjaszewski, Temperature effect on activation rate constants in ATRP: new mechanistic insights into the activation process, *Macromolecules*, 2009, **42**(16), 6050–6055.

36 W. Huang, J.-B. Kim, M. L. Bruening and G. L. Baker, Functionalization of surfaces by water-accelerated atom-transfer radical polymerization of hydroxyethyl methacrylate and subsequent derivatization, *Macromolecules*, 2002, **35**(4), 1175–1179.

37 N. V. Tsarevsky, T. Pintauer and K. Matyjaszewski, Deactivation efficiency and degree of control over polymerization in ATRP in protic solvents, *Macromolecules*, 2004, **37**(26), 9768–9778.

38 M. Fantin, A. A. Isse, A. Gennaro and K. Matyjaszewski, Understanding the fundamentals of aqueous ATRP and defining conditions for better control, *Macromolecules*, 2015, **48**(19), 6862–6875.

39 S. B. Lee, A. J. Russell and K. Matyjaszewski, ATRP synthesis of amphiphilic random, gradient, and block copolymers of 2-(dimethylamino) ethyl methacrylate and n-butyl methacrylate in aqueous media, *Biomacromolecules*, 2003, **4**(5), 1386–1393.

40 C. Li, N. J. Buurma, I. Haq, C. Turner, S. P. Armes, V. Castelletto, I. W. Hamley and A. L. Lewis, Synthesis and characterization of biocompatible, thermoresponsive ABC and ABA triblock copolymer gelators, *Langmuir*, 2005, **21**(24), 11026–11033.

41 H. G. Börner, K. Beers, K. Matyjaszewski, S. S. Sheiko and M. Möller, Synthesis of molecular brushes with block copolymer side chains using atom transfer radical polymerization, *Macromolecules*, 2001, **34**(13), 4375–4383.

42 A. P. Narrainen, S. Pascual and D. M. Haddleton, Amphiphilic diblock, triblock, and star block copolymers by living radical polymerization: Synthesis and aggregation behavior, *J. Polym. Sci., Part A: Polym. Chem.*, 2002, **40**(4), 439–450.

43 M. Ouchi, T. Terashima and M. Sawamoto, Transition metal-catalyzed living radical polymerization: toward perfection in catalysis and precision polymer synthesis, *Chem. Rev.*, 2009, **109**(11), 4963–5050.

44 M. Divandari, E. S. Dehghani, N. D. Spencer, S. N. Ramakrishna and E. M. Benetti, Understanding the effect of hydrophobic protecting blocks on the stability and biopassivity of polymer brushes in aqueous environments: A Tiramisu for cell-culture applications, *Polymer*, 2016, **98**, 470–480.

45 K. Matyjaszewski, P. J. Miller, N. Shukla, B. Immaraporn, A. Gelman, B. B. Luokala, T. M. Siclovan, G. Kickelbick, T. Vallant and H. Hoffmann, Polymers at interfaces: using atom transfer radical polymerization in the controlled growth of homopolymers and block copolymers from silicon surfaces in the absence of untethered sacrificial initiator, *Macromolecules*, 1999, **32**(26), 8716–8724.

46 J.-B. Kim, W. Huang, M. L. Bruening and G. L. Baker, Synthesis of triblock copolymer brushes by surface-initiated atom transfer radical polymerization, *Macromolecules*, 2002, **35**(14), 5410–5416.

47 A. Li, S. N. Ramakrishna, P. C. Nalam, E. M. Benetti and N. D. Spencer, Stratified polymer grafts: synthesis and characterization of layered ‘brush’ and ‘gel’ structures, *Adv. Mater. Interfaces*, 2014, **1**(1), 1300007.

